

Preparation and study of structure, electric transport and magnetic properties of $\text{Sr}_3\text{Ru}_2\text{O}_7$ and $\text{Sr}_3\text{Ru}_{1.5}\text{Fe}_{0.5}\text{O}_7$

INDU B SHARMA* and DEVINDER SINGH

Department of Chemistry, University of Jammu, Jammu 180 004, India

MS received 12 March 1996; revised 7 July 1996

Abstract. $\text{Sr}_3\text{Ru}_2\text{O}_7$ and $\text{Sr}_3\text{Ru}_{1.5}\text{Fe}_{0.5}\text{O}_7$ have been prepared by the ceramic method. XRD studies show that the phases crystallize as tetragonal unit cells with the space group $I4/mmm$. Electric conduction in these phases follows variable range-hopping mechanism but the characteristic energy of hopping in $\text{Sr}_3\text{Ru}_2\text{O}_7$ is reduced to a great extent. Magnetic susceptibility of $\text{Sr}_3\text{Ru}_2\text{O}_7$ shows an abrupt rise below 200 K. $\text{Sr}_3\text{Ru}_{1.5}\text{Fe}_{0.5}\text{O}_7$ is antiferromagnetic.

Keywords. $\text{Sr}_3\text{Ru}_2\text{O}_7$; $\text{Sr}_3\text{Ru}_{1.5}\text{Fe}_{0.5}\text{O}_7$; electric transport; magnetic properties.

1. Introduction

Many Ruddlesden–Popper (RP) type compounds with composition $\text{A}_{n+1}\text{B}_n\text{O}_{3n+1}$ are known (Ruddlesden and Popper 1958; Mohan Ram *et al* 1986; Sreedhar *et al* 1994; Zhang *et al* 1994). The composition of such phases could also be expressed as $\text{AO}(\text{ABO}_3)_n$, where n perovskite slabs are stacked between the rock salt-like AO layers along the crystallographic c -axis. The $n = 1$ phases, with K_2NiF_4 -type structure, possess two-dimensional character. Three-dimensional character increases in higher members of an RP-family because of increase in the number of ABO_3 slabs. Increase in n is expected to increase the strength of B–O–B interactions along the crystallographic c -axis. In case A is a rare-earth or alkaline earth ion and B is a transition metal ion, their electric transport and magnetic properties become interesting and within a series, these properties are governed by the identity and valence state of the ions, width of n perovskite slabs and oxygen content.

In the RP-family $\text{Sr}_{n+1}\text{Ru}_n\text{O}_{3n+1}$, formation and characterisation of some members are reported in the literature (Randall and Ward 1959; Kafalas and Longo 1972; Rao *et al* 1988; Huang *et al* 1994). Sr_2RuO_4 is reported to be antiferromagnetic, while the $n = \infty$ member is a ferromagnetic conductor. The $n = 2$ member is synthesised from $\text{Sr}_2\text{RuO}_4 \cdot 0.25\text{CO}_2$ by its treatment with RuO_2 and is shown to be a metallic conductor down to 4 K (Cava *et al* 1995). In the present work, $\text{Sr}_3\text{Ru}_2\text{O}_7$ has been prepared by the traditional ceramic method, its structural parameters have been computed by X-ray diffractometry, and the electric transport and magnetic properties have been followed as functions of temperature. Effect of partial replacement of ruthenium ion by iron on structure, electronic conduction and magnetic properties has also been studied.

* For correspondence

Table 1. Powder X-ray diffraction data of $\text{Sr}_3\text{Ru}_2\text{O}_7$ (space group $I4/mmm$).
 $a = 3.894 \text{ \AA}$; $c = 20.705 \text{ \AA}$

h	k	l	$d_{\text{obs}}(\text{\AA})$	$d_{\text{cal}}(\text{\AA})$	I_{obs}	I_{cal}
0	0	4	5.155	5.176	6	10
1	0	1	3.817	3.826	5	3
1	0	5	2.831	2.836	100	100
1	1	0	2.763	2.753	66	59
1	0	7	2.356	2.355	6	6
0	0	10	2.067	2.070	13	16
2	0	0	1.949	1.947	39	37
0	0	12	1.728	1.725	27	28
1	1	10	1.655	1.655	17	19
2	1	5	1.605	1.605	44	43
2	0	10	1.417	1.418	13	21
2	2	0	1.378	1.377	9	13

Table 2. Powder X-ray diffraction data of $\text{Sr}_3\text{Ru}_{1.5}\text{Fe}_{0.5}\text{O}_7$ (space group $I4/mmm$).
 $a = 3.910 \text{ \AA}$; $c = 20.342 \text{ \AA}$

h	k	l	$d_{\text{obs}}(\text{\AA})$	$d_{\text{cal}}(\text{\AA})$	I_{obs}
0	0	4	5.107	5.085	8
1	0	1	3.838	3.839	8
1	0	5	2.819	2.819	100
1	1	0	2.765	2.765	80
1	1	6	2.145	2.142	10
0	0	10	2.038	2.034	14
2	0	0	1.955	1.955	40
1	0	11	1.671	1.762	8
1	1	10	1.642	1.638	12
2	1	5	1.607	1.606	33
1	1	12	1.447	1.445	7
2	0	10	1.411	1.409	11
2	2	0	1.383	1.382	11
2	2	2	1.372	1.370	7

2. Experimental

2.1 Preparation and analysis

AR grade SrCO_3 , RuO_2 and Fe_2O_3 (of purity > 99.9%) were used as starting materials. The reactant powdered oxides were weighed in ratios corresponding to the stoichiometry of the desired phases, homogenized by grinding and mixing, pressed into pellets and heat-treated at 1573 K in static air atmosphere for at least 40 h with a number of intermediate grindings and pelletizings. The black coloured products were finally pulverized and analysed by usual chemical methods for the constituent cations. The compounds were heated in a stream of 10% H_2 + 90% N_2 up to 1270 K and weighed both before and after heating. Assuming the products to be SrO + ruthenium

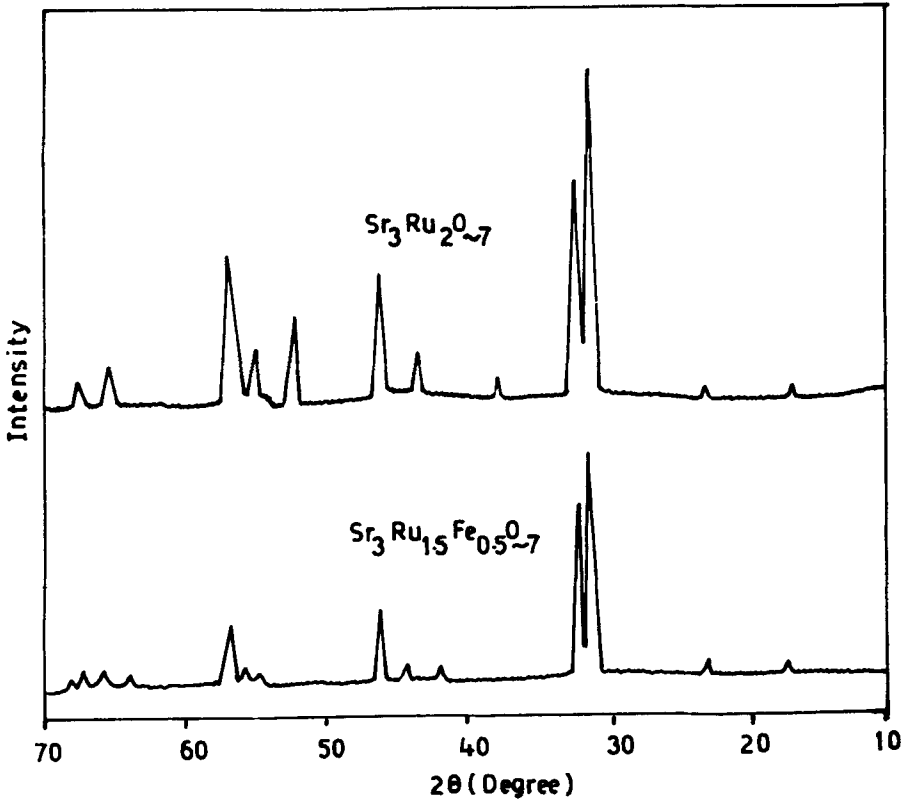


Figure 1. X-ray diffraction patterns of $\text{Sr}_3\text{Ru}_2\text{O}_7$.

metal in the Sr–Ru–O phase and SrO + ruthenium metal + iron metal in the Sr–Ru–Fe–O phase, the oxygen content was calculated. The results correspond to $\text{Sr}_3\text{Ru}_2\text{O}_7$ and $\text{Sr}_3\text{Ru}_{1.5}\text{Fe}_{0.5}\text{O}_7$ stoichiometries.

2.2 XRD studies

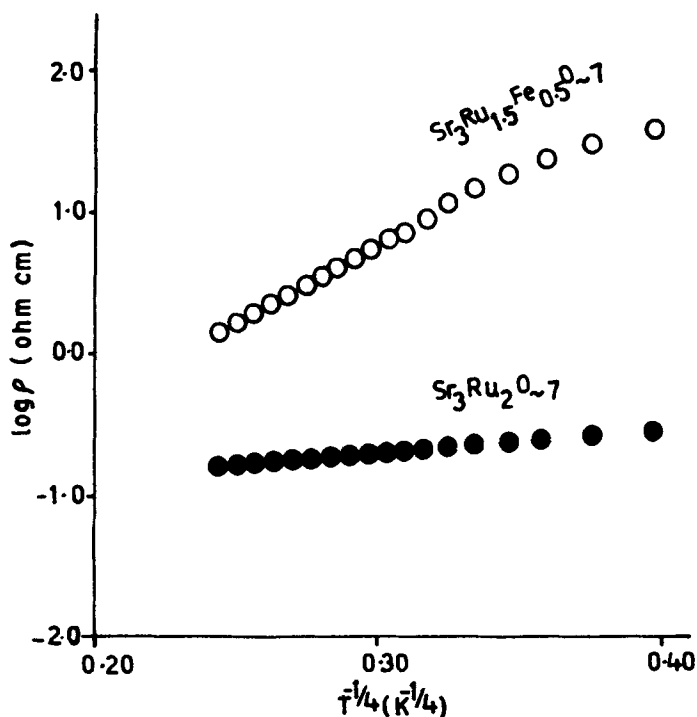
Room temperature powder X-ray diffraction data of the phases were recorded on a Philips diffractometer type PW 1050/71 at a scanning speed of $1^\circ/\text{minute}$ using CuK_α radiations. The data are given in tables 1 and 2, while the patterns are plotted in figure 1.

2.3 Electric transport and magnetic susceptibility measurements

Electrical resistivity of the sintered pellets of the phases was measured by the four-probe method in the temperature range of 10–300 K using a Leybold closed-cycle helium cryostat, a Keithley nanovoltmeter and a constant current source. For electrodes thin copper wires attached to the surface of the pellets with silver paste were used. Magnetic susceptibilities of the polycrystalline samples were measured by the Faraday technique in the temperature region 77–300 K using $\text{HgCo}(\text{SCN})_4$ as calibrant in an external field of 3,700 gauss. All magnetic susceptibility values were corrected for diamagnetism of the constituent atoms.

Table 3. Positional co-ordinates of Sr, Ru and O in $\text{Sr}_3\text{Ru}_2\text{O}_7$.

Atom	x	y	z
Sr(1)	0.0	0.0	0.5
Sr(2)	0.0	0.0	0.315
Ru	0.0	0.0	0.097
O(1)	0.0	0.0	0.0
O(2)	0.0	0.0	0.190
O(3)	0.0	0.50	0.096

**Figure 2.** Plot of $\log \rho$ versus T .

3. Results and discussion

The X-ray diffraction data of $\text{Sr}_3\text{Ru}_2\text{O}_7$ (table 1 and figure 1) could be indexed on the basis of the tetragonal unit cell with $a = 3.894 \text{ \AA}$ and $c = 20.705 \text{ \AA}$. Theoretical diffraction intensities of this phase have been calculated with the Lazy-Pulverix computer program based on these cell parameters, $I4/mmm$ space group and the atomic positions given in table 3. Comparison of the calculated and experimental intensities, table 1, shows good agreement considering that preferred orientation effects are neglected. The XRD data for $\text{Sr}_3\text{Ru}_{1.5}\text{Fe}_{0.5}\text{O}_7$ (table 2 and figure 1) have been indexed for tetragonal unit cell with $a = 3.910 \text{ \AA}$ and $c = 20.342 \text{ \AA}$. The shrinkage in the unit cell volume with partial replacement of ruthenium by iron is in accordance with the ionic size of the two. The XRD intensity pattern of this phase resembles that of $\text{Sr}_3\text{Ru}_2\text{O}_7$.

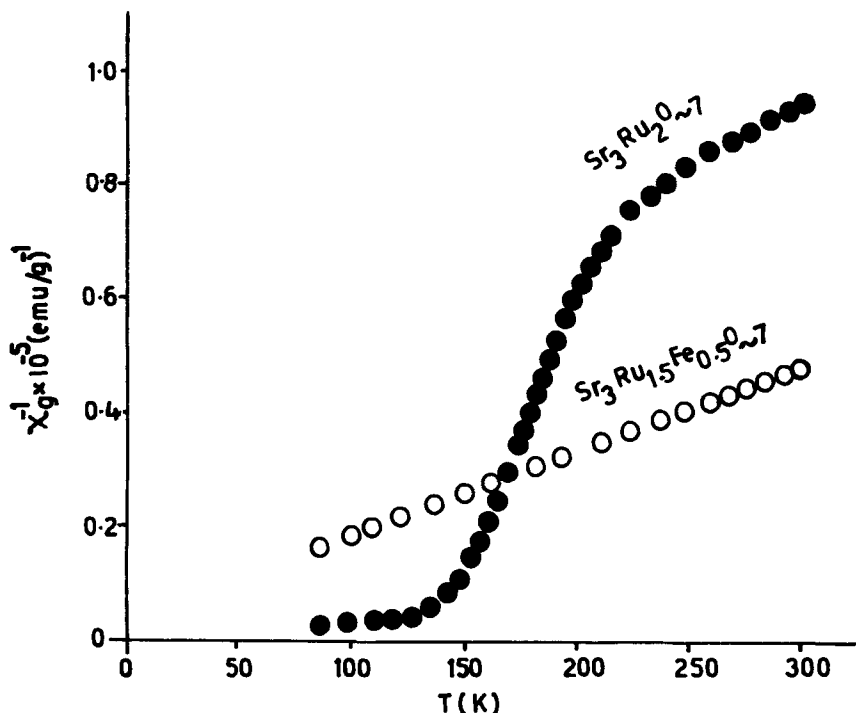


Figure 3. Plot of χ_g^{-1} versus T .

Electrical resistivity data for $\text{Sr}_3\text{Ru}_2\text{O}_7$ and $\text{Sr}_3\text{Ru}_{1.5}\text{Fe}_{0.5}\text{O}_7$ show that the temperature coefficients of resistivity (TCR) of both the phases are negative. Linearity of plots between $\log \rho$ and $T^{-1/4}$ (figure 2) shows that the three-dimensional variable range-hopping (VRH) mechanism, expressed by, $\rho = \rho_0 \exp(B/T^{1/4})$, is applicable to electrical conduction. However, deviations from VRH law are observed at low temperatures. The characteristic energy of hopping (B), calculated from the slopes of $\log \rho$ versus $T^{-1/4}$ plots in figure 2 in the higher temperature region, is equal to 5.113 and 28.350 $\text{K}^{1/4}$ for $\text{Sr}_3\text{Ru}_2\text{O}_7$ and $\text{Sr}_3\text{Ru}_{1.5}\text{Fe}_{0.5}\text{O}_7$ respectively. The comparatively large value of B for the mixed Ru/Fe phase suggests that insulator behaviour is more pronounced. This character is much reduced in $\text{Sr}_3\text{Ru}_2\text{O}_7$ because of low value of B , as the materials with values of B approaching zero assume metallic form (Kim *et al* 1992).

The temperature dependence of inverse gram magnetic susceptibility is plotted in figure 3. The plot for $\text{Sr}_3\text{Ru}_2\text{O}_7$ shows that there is steep rise in magnetic susceptibility below 200 K and this behaviour persists up to 140 K. Although X-ray diffraction data of this phase do not show the presence of any impurities, the magnetic behaviour suggests that a small quantity of perovskite impurity (SrRuO_3) is present below the detection limits of the X-ray diffractometer (1–2 vol %), which is responsible for the rise in magnetic susceptibility. Such behaviour for the $n = 1$ and 2 phases has been reported earlier also (Rao *et al* 1988; Cava *et al* 1995). The χ_g^{-1} versus T plot for $\text{Sr}_3\text{Ru}_{1.5}\text{Fe}_{0.5}\text{O}_7$ (figure 3) is linear throughout the temperature region 77–300 K and shows no anomaly. The paramagnetic Curie temperature (θ) is around -20 K which suggests that antiferromagnetic interactions are predominant in this phase.

The experimental Curie constant/magnetic ion (C_{obs}) for $\text{Sr}_3\text{Ru}_{1.5}\text{Fe}_{0.5}\text{O}_7$ has been estimated from χ_M^{-1} versus T plot and is about 1.90 emu K. The theoretical value of the Curie constant has been calculated from the relations:

$$\mu_{\text{cal}}^2 \text{ (magnetic moment)} = X_1 \mu_{\text{Ru}^{5+}}^2 + X_2 \mu_{\text{Ru}^{4+}}^2 + X_3 \mu_{\text{Fe}^{3+}}^2 \quad (1)$$

and

$$C_{\text{cal}} = [\mu_{\text{cal}}/2.828]^2, \quad (2)$$

where the X 's are the molar fractions of the respective ions, while $\mu_{\text{Ru}^{5+}}$, $\mu_{\text{Ru}^{4+}}$ and $\mu_{\text{Fe}^{3+}}$ are the theoretical magnetic moments of Ru^{5+} (low spin state $-t_{2g}^3 e_g^0$), Ru^{4+} (low spin state $-t_{2g}^4 e_g^0$) and Fe^{3+} (high spin state $-t_{2g}^3 e_g^2$) respectively. C_{cal} comes to 2.06 emu K per magnetic ion. Comparison of C_{obs} and C_{cal} shows good agreement especially in view of the fact that antiferromagnetic interactions are predominant.

Acknowledgements

Thanks are due to the Department of Science and Technology, New Delhi for financial support; and the Regional Sophisticated Instrumentation Centre, Chandigarh for recording XRD patterns.

References

- Cava R J, Zandbergen H W, Krajewski J J, Peck W F Jr, Batlogg B, Carter S, Fleming R M, Zhou O and Rupp L W Jr 1995 *J. Solid State Chem.* **116** 141
 Huang Q, Soubeyroux J L, Chaissem O, Sora N, Santoro A, Cava R J, Krajewski J J and Peck W F Jr 1994 *J. Solid State Chem.* **112** 355
 Kafalas J A and Longo J M 1972 *J. Solid State Chem.* **4** 55
 Kim I, Itoh M and Nakamura T 1992 *J. Solid State Chem.* **101** 77
 Mohan Ram R A, Ganapathy L, Ganguly P and Rao C N R 1986 *J. Solid State Chem.* **63** 139
 Randall J J and Ward R 1959 *J. Am. Chem. Soc.* **81** 2629
 Rao C N R, Ganguly P, Singh K K and Mohan Ram R A 1988 *J. Solid State Chem.* **72** 14
 Ruddlesden S N and Popper P 1958 *Acta Cryst.* **11** 54
 Sreedhar K, McElfresh M, Perry D, Kim D, Metcalf P and Honig J M 1994 *J. Solid State Chem.* **110** 208
 Zhang Z, Greenblatt M and Goodenough J B 1994 *J. Solid State Chem.* **108** 402